2016

Electron Shock Waves with a Large Current Behind the Shock Front

H. D. Newberry
Arkansas Tech University, mhemmati@atu.edu

M. Hemmati
Arkansas Tech University

H. D. Moore
Arkansas Tech University

K. Ledbetter
Arkansas Tech University

M. W. Bowman
Arkansas Tech University

Follow this and additional works at: http://scholarworks.uark.edu/jaas

Part of the Fluid Dynamics Commons

Electron Shock Waves with a Large Current behind the Shock Front

H.D. Newberry, M. Hemmati*, H.D. Moore, K. Ledbetter, and M.W. Bowman

Arkansas Tech University, Department of Physical Science, Russellville, AR 72801, USA

Correspondence: mhemmati@atu.edu

Running Title: Electron Shock Waves with a Large Current behind the Shock Front

Abstract

The propagation of breakdown waves in a gas, which is primarily driven by electron gas pressure, is described by a one-dimensional, steady-state, three-component (electrons, ions, and neutral particles) fluid model. We consider the electron gas partial pressure to be much larger than that of the other species and the waves to have a shock front. Our set of equations consists of the equations of conservation of the flux of mass, momentum, and energy coupled with Poisson's equation. This set of equations is referred to as the electron fluid dynamical equations. In this study we are considering breakdown waves propagating in the opposite direction of the electric field force on electrons (return stroke in lightning) and moving into a neutral medium.

For Breakdown waves with a significant current behind the shock front, the set of electron fluid dynamical equations and also the boundary condition on electron temperature need to be modified. For a range of experimentally observed current values and also some larger current values which few experimentalists have been able to observe, we have been able to solve the set of electron fluid dynamical equations through the dynamical transition region of the wave. Some experimentalists have reported the existence of a relationship between return stroke lightning wave speed and current behind the shock front; however, some others are skeptical of the existence of such a relationship. Our solutions to the set of electron fluid dynamical equations within the dynamical transition region of the wave confirm the existence of such a relationship. We will present the method of solution of the set of electron fluid dynamical equations through the dynamical transition region of the wave and also the wave profile for electric field, electron velocity, electron temperature and electron number density, within the dynamical transition region of the wave.

Introduction

Electron shock waves, also known as breakdown waves, were first observed in the form of lightning and studied in laboratory discharge tubes. The phenomenon occurs when the potential difference between two points is high enough to ionize some of the neutral particles and later accelerate the resulting electrons to generate an avalanche-like shock wave. This process converts an ion-less gas into a neutral plasma and results in a high temperature electron gas that expands rapidly to produce an electron shock wave. The emitted radiation has been found to have no Doppler shift; therefore, the ions have no significant mass motion through the wave. When the net electric field force on electrons, applied plus space charge field force, acts in the same direction as the propagation of the wave, the wave is referred to as a pro-force wave. Waves for which the electric field force on electrons is in the opposite direction as the wave propagation are labeled, by definition, as anti-force waves. In the case of anti-force waves, the electron gas temperature, and therefore electron gas partial pressure, is large enough to provide the driving force for the propagation of the wave.

The breakdown wave can be broken into two distinct regions: the Debye sheath region and the quasi-neutral region. The Debye sheath region is a thin, dynamical region that follows the shock front. In the sheath region, the net electric field starts at its maximum value at the shock front and reduces to a negligible value at the trailing end of the sheath. Also electrons, starting from an initial speed behind the shock front, slow down to a speed comparable to that of heavy particles. Following the sheath region of the wave, exists a much longer region referred to as the quasi-neutral region of the wave. In the quasi-neutral region, the electron gas cools down through further ionization of the neutral particles, and ion and electron densities become approximately equal.

H.D. Newberry, M. Hemmati, H.D. Moore, K. Ledbetter, and M.W. Bowman

Model

Paxton and Fowler (1962) were first to formulate a fluid model for breakdown waves which led to a one-dimensional, three component, steady state theory that described breakdown waves propagating into a non-ionized media and in the direction of the electric field force on electrons. The set of equations included conservation of mass, momentum, and energy, and their solutions for the set of equations presented some success. Prior to 1984, Fowler and his associates (1968) added Poisson's equation to the set of fluid equations developed by Paxton (1962), and were able to solve their set of equations using an approximation method. The approximate solutions for the more developed set of equations showed better agreement with experimental results than those presented by Paxton (1962). In the approximate solutions to the set of equations, to make solutions possible, many terms were neglected from the equation of conservation of energy. Fowler et al. (1984) added the previously neglected terms into the equation of conservation of energy, particularly the heat conduction term, which altered the boundary condition on electron velocity and proved to be essential in an exact numerical solution of the set of electron fluid dynamical equations within the dynamical transitional region of the wave. Fowler et al. (1984) complete set of equations for breakdown waves propagating into a non-ionized medium and in the direction of the electric field force on electrons is as follows

$$\frac{d(nv)}{dx} = \beta n \tag{1}$$

$$\frac{d}{dx}[\,nmv(v-V) + nkT_e\,] = -enE - Kmn(v-V) \tag{2}$$

$$\frac{d}{dx}\left(nmv(v-V)^2 + nkT_e(5v-2V) + 2e\phi nv\right. \tag{3}$$
$$\left. - \frac{5nk^2 T_e}{mk}\frac{dT_e}{dx}\right) = -3\left(\frac{m}{M}\right)nKkT_e - \left(\frac{m}{M}\right)nmK(v-V)^2$$

$$\frac{dE}{dx} = \frac{en}{\epsilon_o}\left(\frac{v}{V} - 1\right) \tag{4}$$

In the above equations, E is the electric field magnitude in the sheath region, M is the neutral particle mass, K is the elastic collision frequency, V is the wave velocity, x is the position within the sheath region, E_o is electric field at the wave front, ϕ is the

ionization potential, and β is the ionization frequency. Also, e, v, m, n, and T_e, are electron charge, velocity, mass, number density, and temperature, respectively. To allow for easier solution of these equations, Fowler et al. (1984) introduced the following set of dimensionless variables for proforce breakdown waves:

$$\eta = \frac{E}{E_0} \qquad \omega = \frac{2m}{M} \qquad \mu = \frac{\beta}{K}$$

$$\xi = \frac{xeE_o}{mV^2} \qquad \psi = \frac{v}{V} \qquad \theta = \frac{T_e k}{2e\phi}$$

$$\nu = \frac{n2e\phi}{\varepsilon_o E_0^2} \qquad \alpha = \frac{2e\phi}{mV^2} \qquad \kappa = \frac{mV}{eE_o}K$$

Where, η, μ and ξ are dimensionless electric field, ionization rate, and position within the sheath region of the wave, respectively. Also, ν, ψ, and θ, are the dimensionless electron number density, velocity, and temperature. α and K are wave parameters. Substituting these dimensionless variables into equations 1-4 yields a set of electron fluid dynamical equations in nondimensional form for proforce waves propagating into a non-ionized media. They are as follows:

$$\frac{d}{d\xi}[\nu\psi] = \kappa\mu\nu \tag{5}$$

$$\frac{d}{d\xi}[\nu\psi(\psi-1) + \alpha\nu\theta] = -\nu\eta - \kappa\nu(\psi-1) \tag{6}$$

$$\frac{d}{d\xi}\left(\nu\psi(\psi-1)^2 + \alpha\nu\theta(5\psi-2) + \alpha\nu\psi\right. \tag{7}$$
$$\left. + \alpha\eta^2 - \frac{5\alpha^2\nu\theta}{\kappa}\frac{d\theta}{d\xi}\right) = -\omega\kappa\nu[3\alpha\theta + (\psi-1)^2]$$

$$\frac{d\eta}{d\xi} = \frac{\nu}{\alpha}(\psi-1) \tag{8}$$

To transform these equations into a set describing antiforce breakdown waves, some modifications are needed. Previously Sanmann and Fowler (1975) approximated solutions for antiforce waves by considering a weak discontinuity at the wave front and used a simple sign change for K and μ. Considering waves to have a shock front, however, Hemmati (1999)

Electron Shock Waves with a Large Current Behind the Shock Front

showed Sanmann's (1975) simple change of variable signs were not accurate. Hemmati (1999) derived a new set of non-dimensional variables for the antiforce case and they are

$$\eta = \frac{E}{E_0},$$
$$\omega = \frac{2m}{M},$$
$$\mu = \frac{\beta}{K},$$
$$\xi = -\frac{xeE_o}{mV^2},$$
$$\psi = \frac{v}{V},$$
$$\theta = -\frac{T_e k}{2e\phi},$$
$$\nu = \frac{n2e\phi}{\varepsilon_o E_o^2},$$
$$\alpha = \frac{2e\phi}{mV^2},$$
$$\kappa = \frac{mV}{eE_o}K$$

After applying these new non dimensional variables, Hemmati's (1999) new set of non-dimensional, electron fluid dynamical equations for antiforce waves become

$$\frac{d}{d\xi}[\nu\psi] = \kappa\mu\nu \qquad (9)$$

$$\frac{d}{d\xi}[\nu\psi(\psi-1) + \alpha\nu\theta] = \nu\eta - \kappa\nu(\psi-1) \qquad (10)$$

$$\frac{d}{d\xi}\left(\nu\psi(\psi-1)^2 + \alpha\nu\theta(5\psi-2) + \alpha\nu\psi\right.$$
$$\left. - \frac{5\alpha^2\nu\theta}{\kappa}\frac{d\theta}{d\xi}\right) = 2\nu\eta(\psi-1) - \omega\kappa\nu[3\alpha\theta + (\psi-1)^2] \qquad (11)$$

$$\frac{d\eta}{d\xi} = -\frac{\nu}{\alpha}(\psi-1) \qquad (12)$$

Hemmati et al. (2011) modified the set of electron fluid dynamical equations to describe antiforce waves (return stroke in lightning) with a significant current behind the shock front. With ion number density, Ni, and ion velocity, Vi, behind the wave front, the current behind the wave front will be

$$I_1 = eN_iV_i - env \qquad (13)$$

Ion velocity is considered to be almost equal to neutral particle speed ($V_i \cong V$) due to lack of experimentally observed Doppler shift. No experimentally observed Doppler shift indicates that both the ions and neutral particles have insignificant speeds in the laboratory frame. Substituting V for V_i and solving for N_i from equation 13 yields

$$N_i = \frac{I_1}{eV} + \frac{nv}{V} \qquad (14)$$

Substituting this into Poisson's equation, and applying the dimensionless variables for antiforce waves results in

$$\frac{d\eta}{d\xi} = \frac{KI_1}{\varepsilon_0 KE_0} - \frac{v}{\alpha}(\Psi - 1) \qquad (15)$$

Poisson's equation is then reduced to

$$\frac{d\eta}{d\xi} = K\iota - \frac{v}{\alpha}(\Psi - 1) \qquad (16)$$

Where $\iota = \frac{I_1}{\varepsilon_0 KE_0}$ represents the dimensionless current. The current values behind the shock front in lightning return stroke are generally in the range of 5 to 30 kA. Using a current value of $I_1 = 10kA$ for lighting return stroke, the elastic collision frequency, K, values from (McDaniel, 1964), and also the values of ε_0, and E_0, one can estimate the value of ι to be of the order of 1.

Solving for $v(\Psi-1)$ from equation (16) and substituting it into the equation of conservation of energy for antiforce waves, equation (11), produces the final form of the equation of conservation of energy for antiforce waves with a large current behind the wave front. This completes the final form of the set of electron fluid dynamical equations describing antiforce waves with a large current behind the shock front

$$\frac{d}{d\xi}[\nu\psi] = \kappa\mu\nu \qquad (17)$$

$$\frac{d}{d\xi}[\nu\psi(\psi-1) + \alpha\nu\theta] = \nu\eta - \kappa\nu(\psi-1) \qquad (18)$$

$$\frac{d}{d\xi}\left(\nu\psi(\psi-1)^2 + \alpha\nu\theta(5\psi-2) + \alpha\nu\psi\right.$$
$$\left. - \frac{5\alpha^2\nu\theta}{\kappa}\frac{d\theta}{d\xi} + \alpha\eta^2\right) = 2\eta\kappa\iota\alpha - \omega\kappa\nu[3\alpha\theta + (\psi-1)^2] \qquad (19)$$

$$\frac{d\eta}{d\xi} = \kappa\iota - \frac{v}{\alpha}(\psi-1) \qquad (20)$$

To solve the set of electron fluid dynamical equations for antiforce waves with a large current behind the shock front, Hemmati et al. (2015) had to modify the initial condition on electron temperature as well. They used the all particle (global) momentum equation to find the shock condition on electron temperature, and in dimensionless form, the electron temperature at the shock front becomes

$$\theta_1 = \frac{\Psi_1(1-\Psi_1)}{\alpha} - \frac{\kappa\iota}{\nu_1}. \qquad (21)$$

H.D. Newberry, M. Hemmati, H.D. Moore, K. Ledbetter, and M.W. Bowman

Results and Discussion

A trial and error technique of integration was used to obtain solutions for our complete set of electron fluid dynamical equations through the dynamical transition (sheath) region of the wave. For a specific wave speed, α, and dimensionless current, ι, a set of values for wave constant, К, electron number density, ν_1, and electron velocity, Ψ_1, at the wave front were chosen, and in integration of the set of equations through the sheath region of the wave, those values were systematically changed until the integration of the set of electron fluid dynamical equations through the sheath region of the wave resulted in a successful conclusion. Meaning that, at the conclusion of the integration of the set of equations, $\Psi_2 \rightarrow 1$, and, $\eta_2 \rightarrow 0$, at the trailing edge of the wave. Integration of our set of electron fluid dynamical equations for higher wave speed values, meaning for small α values, is not very challenging; therefore, we intended to find solutions for lower ranges of wave speed values. For a certain wave speed value, α, integration of the set of electron fluid dynamical equations through the sheath region of the wave for small dimensionless current values, ι, also is relatively straight forward; however, as the dimensionless current value increases, the sheath thickness increases as well and the integration of the set of equations through the sheath region becomes more involved and time consuming. For a specific wave speed value, we intended to find the largest current value for which integration of the set of electron fluid dynamical equations through the sheath region of the wave became possible. For four wave speed values shown below and for the largest dimensionless current values for which integration of the set of electron fluid dynamical equations through the sheath region of the wave, for respective wave speeds became possible, the following set of initial boundary values and wave constants had to be employed.

$\alpha = 1 \quad \iota = 0.5 \quad$ К$= 0.1338 \quad \nu_1 = 0.4882 \; \Psi_1 = 0.5502$

$\alpha = 0.25 \; \iota = 1 \quad$ К$= 0.33 \quad \nu_1 = 0.81 \quad \Psi_1 = 0.85$

$\alpha = 0.05 \quad \iota = 2 \quad$ К$= 0.6 \quad \nu_1 = 0.7655 \; \Psi_1 = 0.8876$

$\alpha = 0.005 \; \iota = 5 \quad$ К$= 1.34 \quad \nu_1 = 0.525 \quad \Psi_1 = 0.5469$

The following figures represent the wave profile for antiforce waves with a significant current behind the shock front. Figures 1 through 3 show that solutions to the set of electron fluid dynamical equations within the sheath region of the wave all have met the required boundary conditions at the trailing edge of the wave ($\Psi_2 \rightarrow 1, \; \eta_2 \rightarrow 0$).

Figure 1 shows dimensionless electric field, η, as a function of dimensionless electron velocity, ψ, within the sheath region of the wave for four values of wave speed, α, and respective dimensionless current values, ι.
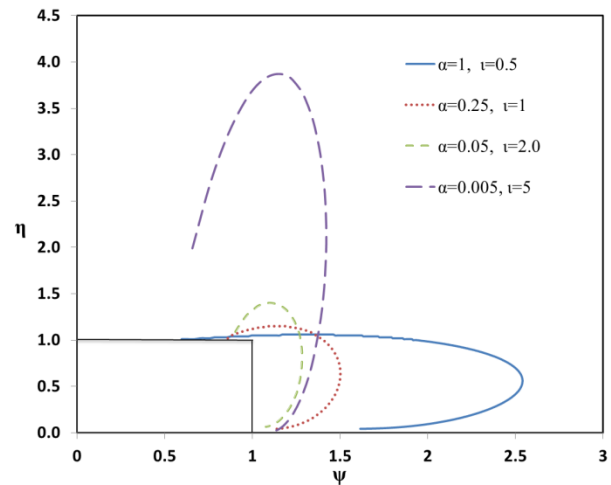

Figure 1. Electric field, η, as a function of electron velocity, ψ, for four dimensionless wave speed values, α, and respective dimensionless current values, ι, of 1, 0.5; 0.25, 1.0; 0.05, 2.0 and 0.005, 5.0 within the sheath region of the wave.

Figure 2 shows dimensionless electric field, η, as a function of dimensionless position, ξ, within the sheath region of the wave for four wave speed values, α, and respective dimensionless current values, ι.
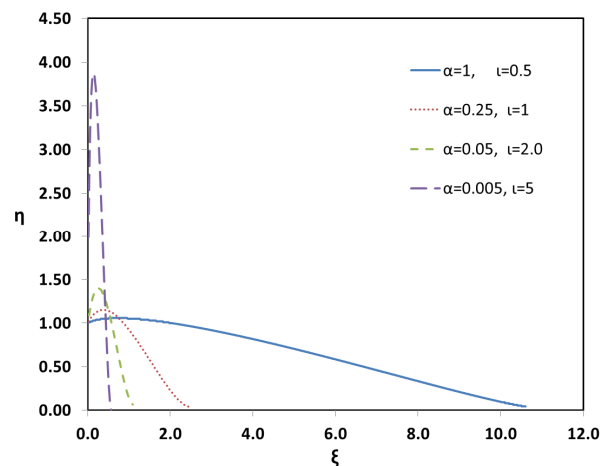

Figure 2. Dimensionless electric field, η, as a function of dimensionless position, ξ, for four wave speed values, α, and respective dimensionless current values, ι, of 1, 0.5; 0.25, 1.0; 0.05, 2.0 and 0.005, 5.0 within the sheath region of the wave.

Electron Shock Waves with a Large Current Behind the Shock Front

Figure 3 shows dimensionless electron velocity, ψ, as a function of dimensionless position within the sheath region of the wave for four wave speed values, α, and respective dimensionless current values, ι.
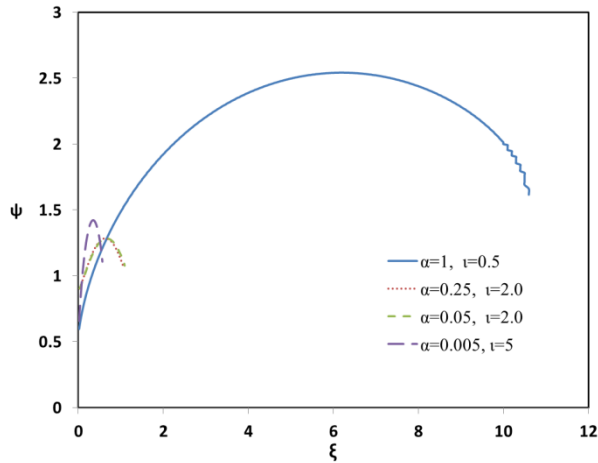

Figure 3. Dimensionless electron velocity, ψ, as a function of dimensionless position, ξ, for four wave speed values, α, and respective dimensionless current values, ι, of 1, 0.5; 0.25, 1.0; 0.05, 2.0 and 0.005, 5.0 within the sheath region of the wave.

Figure 4 shows dimensionless electron number density, υ, as a function of dimensionless position, ξ, within the sheath region of the wave for four wave speed values, α, and respective dimensionless current values, ι.
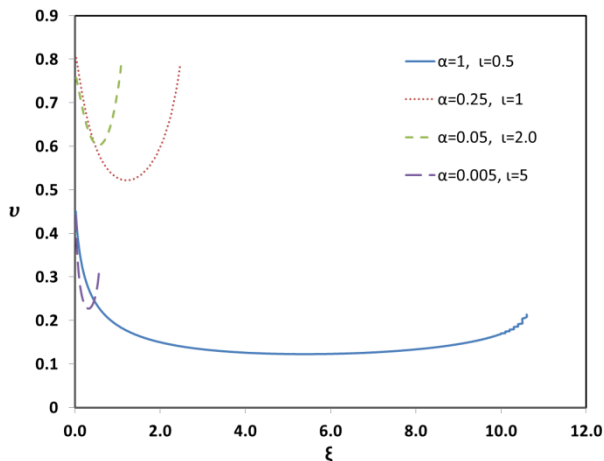

Figure 4. Dimensionless electron number density, υ, as a function of dimensionless position, ξ, for four dimensionless wave speed values, α, and respective dimensionless current values, ι, of 1, 0.5; 0.25, 1.0; 0.05, 2.0 and 0.005, 5.0 within the sheath region of the wave.

Figure 5 shows dimensionless electron temperature, θ, as a function of dimensionless position, ξ, within the sheath region of the wave for four wave speed values, α, and respective dimensionless values, ι, graphed with a logarithmic scale on the y axis. α =0.005 represents a relatively fast wave speed value of 4.2×10^7 m/s, and α = 1 represents slow wave speed value of 3×10^6 m/s. Short dimensionless sheath thickness, ξ, value of, 0.56 represents an actual sheath thickness of 5.6 mm
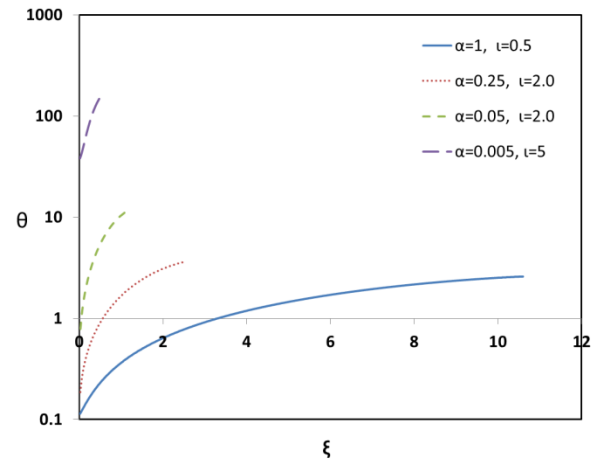

Figure 5. Dimensionless electron temperature, θ, as a function of dimensionless position, ξ, for four wave speed values, α, and respective dimensionless current values, ι, of 1, 0.5; 0.25, 1.0; 0.05, 2.0 and 0.005, 5.0 within the sheath region of the wave.

Researchers have debated the possible existence of a relationship between wave speed values and peak current values in lightning return strokes. For instance, Wagner (1963) has suggested that as the lightning return stroke wave speed increases, it can support larger peak current values; but others, notably Mach and Rust (1989) disagree, claiming a lack of correlation between return stroke propagation speed and peak current. Our solutions indicate that a relationship does exist, as the lightning return stroke speed increases, it can support higher peak current values.

Investigators, for example, Rakov (2007), have reported minimum wave speeds for lightning return stroke typically to be in the order of 10^7 m/s. However, as we indicated above, we have been able to integrate our set of electron fluid dynamical equations through the sheath region of the wave for lightning return stroke speeds as low as 3×10^6 m/s. Thus, our model predicts that antiforce waves with wave speeds below that of those experimentally measured can be detected.

Conclusions

Our modified set of electron fluid dynamical equations for antiforce waves with a large current behind the wave front, with modified electron temperature at the shock front, have been utilized in our integration of the set of electron fluid dynamical equations through the sheath region of the wave. Our solutions for several wave speed values, with maximum currents possible for the selected wave speeds, all meet the expected physical conditions at the trailing edge of the dynamical transition region of the wave. This indicates validity of our modified set of electron fluid dynamical equations and the extent and possible range of wave speed values and currents for lightning return strokes. Our solutions indicate that lightning return stroke speeds lower than the ranges reported by the majority of experimentalists are also possible. Our solutions also indicate, for lightning return stroke, as the wave speed increases, it can support larger currents behind the shock front. This means that in a lightning return stroke, a relationship between the wave speed values and peak currents exists.

Acknowledgements

Literature Cited

Fowler RG, M Hemmati, RP Scott and **S Parsendajadh**. 1984. Electric breakdown waves: Exact numerical solutions. Part 1. The Physics of Fluids 27(6):1521-1526

Hemmati M, W Childs, H Shojaei and **D Waters**. 2011. Antiforce Current Bearing Waves. Proceedings of 28th International Symposium on Shock Waves. (ISSW28), July 2011, England.

Hemmati M, W Childs, H Shojaei and **RS Horn**. 2015. Wave Profile and Current limits for lightning return stroke. Proceedings of 30th International Symposium on Shock Waves. (ISSW30), July 2015, Israel.

Hemmati M. 1999. Electron Shock Waves: Speed Range for Antiforce Waves. Proceedings of 22nd International Symposium on Shock Waves. Pp. 995-1000.

Mach DM and **WD Rust**. 1989a. Photoelectric return stroke velocity and peak current estimates in natural and triggered lightning, Journal of Geophysics Research 94: 13,237-47.

McDaniel EW. 1964. Collision phenomena in ionized gases, (Wiley, New York)

Paxton GW and **RG Fowler**. 1962. Theory of breakdown wave propagation. Physical Review 128(3):993-997

Rakov VA. 2007. Lightning Return Stroke Speed. Journal of Lightning Research 1:80-89.

Shelton GA and **RG Fowler**. (1968). Nature of electron-fluid-dynamical waves. The Physics of Fluids 11(4):740-746.

Sanmann E and **RG Fowler**. 1975. Structure of electron fluid dynamical plane waves: Antiforce waves. The Physics of Fluids 18(11):1433-1438.

Wagner CF. 1963. Relation between stroke current and velocity of return stroke. IEEE Transactions on Power Apparatus and Systems. 82:609-17.